

# Novel low-temperature sintering ceramic substrate based on indialite/cordierite glass ceramics

Jobin Varghese<sup>\*1</sup>, Timo Vahera<sup>1</sup>, Hitoshi Ohsato<sup>1,2</sup>, Makoto Iwata,<sup>3</sup> and Heli Jantunen<sup>1</sup>

<sup>1</sup>Microelectronics Research Unit, Faculty of Information Technology and Electrical Engineering,  
University of Oulu, Oulu 90014, Finland

<sup>2</sup>Nagoya Industrial Science Research Institute, Nagoya 464-0819, Japan

<sup>3</sup>Nagoya Institute of Technology, Nagoya 466-8555, Japan

## Abstract

In this paper, a novel low-temperature sintering substrate for low temperature co-fired ceramic applications based on indialite/cordierite glass ceramics with Bi<sub>2</sub>O<sub>3</sub> as a sintering aid showing low permittivity ( $\epsilon_r$ ) and ultralow dielectric loss ( $\tan\delta$ ) is described. The fine powder of indialite was prepared by the crystallization of cordierite glass at 1000 °C/1 h. The optimized sintering temperature was 900 °C with 10 wt% Bi<sub>2</sub>O<sub>3</sub> addition. The relative density achieved was 97%, and  $\epsilon_r$  and  $\tan\delta$  were 6.10 and 0.0001 at 1 MHz, respectively. The composition also showed a moderately low temperature coefficient of relative permittivity of 118 ppm/°C at 1 MHz. The obtained linear coefficient of thermal expansion was 3.5 ppm/°C in the measured temperature range of 100-600 °C. The decreasing trend in dielectric loss, the low relative permittivity at 1 MHz, and the low thermal expansion of the newly developed composition make it an ideal choice for radio frequency applications.

## 1. Introduction

Recently, low-temperature cofired ceramic (LTCC) materials have combined the advantages of multilayer ceramic and thick film technologies to meet the increasing need for electronics running at extreme operating temperatures and in other harsh environments.<sup>1-5)</sup> The low dielectric loss characteristics of the LTCC make it an excellent choice for high-frequency applications and enable circuits and devices that are more efficient.<sup>6-15)</sup> These materials should have low permittivity ( $\epsilon_r < 10$ ), low dielectric loss ( $\tan \delta \sim 10^{-3}$ ), and a low-temperature dependence of resonant frequency ( $TCf < 20 \text{ ppm}/^\circ\text{C}$ ).<sup>3, 16-18)</sup> This is because the low relative permittivity increases the signal speed<sup>3, 19-23)</sup>, and the low dielectric loss minimizes the insertion loss and enables highly selective circuits and applications.<sup>3, 24-25)</sup> Furthermore, the near-zero temperature stability of dielectric properties enables the frequency and insertion loss stability of the devices.<sup>26-28)</sup>

Ohsato *et al.*<sup>29)</sup> reported in 2011 indialite/cordierite ( $\text{Mg}_2\text{Al}_4\text{Si}_5\text{O}_{18}$ ) glass ceramics crystallized at 1200 to 1400 °C for 10 and 20 h. Indialite/cordierite is one of the silicates reported to have excellent properties being suitable for microwave and millimeter-wave applications owing to its low relative permittivity ( $\epsilon_r$  of 4.7) and high quality factor ( $Qf > 200,000 \text{ GHz}$ ).<sup>30)</sup> However, the high crystallization temperature of these glass ceramics limits their feasibility to LTCC packages. This paper focus on the development of indialite/cordierite glass ceramics with  $\text{Bi}_2\text{O}_3$  as the sintering aid, which provides liquid-phase-assisted densification for the developed LTCC substrates. The paper also describes the tape casting, firing, and dielectric properties of the developed LTCC composition.

## 2. Experimental methods

The primary cordierite/indialite  $\text{Mg}_2\text{Al}_4\text{Si}_5\text{O}_{18}$  composition was based on Ohsato's previously published article.<sup>30)</sup> The composition was melted at 1550 °C, refined at 1600 °C/1 h, and crushed roughly to a particle size below 1mm. This was followed by the crystallization of the indialite phase at 1000 °C/1 h<sup>31)</sup> and ball milling to reduce the particle size. The sintering aid  $\text{Bi}_2\text{O}_3$  (high-purity (99%)  $\text{Bi}_2\text{O}_3$ ; Alfa Aesar) was added at 5, 10, 15, and 20 wt% to the processed indialite powder,

followed by pelletization using a 14 mm diameter tungsten carbide cylindrical die with a pressure of 100 MPa from a uniaxial pressing unit. The initial particle size and surface area analyses of the powder were performed using the laser diffraction method (Beckman Coulter, LS13320) as well as a particle surface area analyzer (G.W. Berg & Co; Micrometrics ASAP 2020). The tape casting slurry was made using xylene (ACS reagent 98.5 wt% xylene ethyl benzene)/ethanol (Etax Aa 99.5 wt% ethanol) as the solvent system, menhaden fish oil (Blown Menhaden fish oil grade Z-3) as the dispersant, poly(vinyl butyral) (PVB; Butvar B98) as the binder, and butyl benzyl phthalate (BBP; Santicizer S160) and poly ethylene glycol (PEG; UCON50HB2000) as plasticizers. The ceramic powder was mixed with the solvent and dispersant by ball milling for around 20 h, followed by the addition of the binder and plasticizers and further milling for approximately 24 h. Finally, the slurry was cast onto a silicone-coated Mylar carrier tape using a 400  $\mu\text{m}$  doctor blade. The cast tape was peeled off the Mylar film, followed by subsequent lamination with uniaxial pressing before binder burnout and sintering.

The crystal structure of the specimen was analyzed by X-ray powder diffraction (XRPD; Bruker D8) using monochromatized Cu K $\alpha$  radiation. The bulk densities of the sintered samples were measured by the Archimedes method. The microstructural analysis of the thermally etched tape samples was performed by scanning electron microscopy (FESEM; Zeiss Ultra Plus). The temperature coefficient of relative permittivity ( $TC\epsilon$ ) was measured using a precision LCR meter (Hewlett-Packard/Agilent Technologies 4284A) with a temperature chamber (Espec; SU-261) in the temperature range of -40 to 100 °C. The relative permittivity and dielectric loss in the frequency range of 100 Hz-1 MHz were measured using the same LCR meter. The coefficient of thermal expansion ( $CTE$ ) was investigated in the temperature range of 100-600 °C with cylindrical samples of 8  $\times$  15 mm<sup>2</sup> dimensions using a dilatometer (NETZSCH DIL 402 PC/4).

### **3. Results and discussion**

Figure 1(a) shows the XRPD patterns of 5, 10, 15, and 20 wt% Bi<sub>2</sub>O<sub>3</sub>-added indialite powder samples sintered at 900 °C for 2 h. The results indicate that, after the addition of 5 wt% Bi<sub>2</sub>O<sub>3</sub>, the major phase is indialite, while with 10-20 wt% addition, the secondary phase Bi<sub>2</sub>SiO<sub>5</sub> appears. All the peaks are indexed with standard ICDD card numbers 01-082-1542 for Mg<sub>2</sub>Bi<sub>0.168</sub>(Al<sub>4</sub>Si<sub>5</sub>O<sub>18</sub>) and 04-019-9380 for Bi<sub>2</sub>SiO<sub>5</sub>. It was observed that, when the Bi<sub>2</sub>O<sub>3</sub> content increased, the Bi<sub>2</sub>SiO<sub>5</sub> phase was more prominent after sintering at 900 °C.

The best dopant level was optimized based on dielectric properties and densification.

Figure 1(b) shows the  $\epsilon_r$  and  $\tan\delta$  of the samples sintered at 900 °C/2 h using 5-20 wt% Bi<sub>2</sub>O<sub>3</sub>-added indialite ceramics at 1 MHz. It is evident from Fig. 1(b) that  $\epsilon_r$  increases from 5.7 to 9.9 and  $\tan\delta$  first decreases from 0.004 to 0.0001 and then increases from 0.0001 to 0.0007 owing to the increasing secondary phase Bi<sub>2</sub>SiO<sub>5</sub>. Thus, the suitable composition from the viewpoint of dielectric properties is achieved by the addition of 10 wt% Bi<sub>2</sub>O<sub>3</sub> with  $\epsilon_r = 6.10$  and  $\tan\delta = 0.0001$  at 1 MHz.

Figure 1(c) shows the densification of 10 wt% Bi<sub>2</sub>O<sub>3</sub>-added indialite at sintering temperatures of 850-950 °C/2 h. The sample sintered at 900 °C showed good densification of 97%. The backscattered electron image of this sample sintered at 900 °C with a high-density microstructure is shown in the inset of Fig. 1(c). Indialite grains are surrounded by bright areas that are detected to be Bi<sub>2</sub>SiO<sub>5</sub> after cooling. Thus, during sintering, Bi<sub>2</sub>O<sub>3</sub> is expected to melt at 830 °C, enabling liquid phase densification<sup>32)</sup>. The Bi<sub>2</sub>SiO<sub>5</sub> phase is also formed by crystallization from the melt that dissolves part of indialite at 900 °C as shown in a Bi<sub>2</sub>O<sub>3</sub>-SiO<sub>2</sub> binary metastable phase diagram by Fei *et al.*<sup>33)</sup> At higher sintering temperatures, the slight decrease in densification may be due to the slight evaporation of Bi<sub>2</sub>O<sub>3</sub> or the secondary phase observed by XRPD. From the dielectric properties and densification measurement results, the low-temperature sintering conditions for substrate fabrication with tape casting were selected to be 10 wt% Bi<sub>2</sub>O<sub>3</sub> and a sintering temperature of 900 °C/2 h.

For the next step, the authors fabricated low-temperature sintering ceramic substrates with 5 layers for LTCC. The initial average particle size of the ceramic mixture (10 wt% Bi<sub>2</sub>O<sub>3</sub>-added indialite) was 2.9 μm, and the single-point surface area at P/P<sub>0</sub> = 0.1998 was 15.52 m<sup>2</sup>/g. From these results, the slurry compositions were calculated as reported earlier.<sup>34)</sup> The final tape casting slurry compositions are shown in Table I.

Figure 2 shows the photographs of the cast green tape (a), five-layers thermally laminated tape (b), and sintered substrate (c). The cast tape had a single layer thickness of about 120-130 μm, which is mechanically stable for further thermolamination postprocessing. Figure 2(b) depicts the thermally laminated five-layer stack before shaping the edges with an approximate thickness of 600 μm. The thermally laminated tape was carefully shaped and sintered at 900 °C/2 h with its optimized sintering temperature. The sintered substrate (c) showed densification with a flat surface and no cracking.

Figure 3(a) shows the cross-sectional microstructure of a peeled off single layer of green tape with an average thickness of 120 μm. A magnified microstructural view in Fig. 3(b) reveals the good packing density of a single-layer green tape with a maximum ceramic mixture loading of 55 wt% surrounded by an organic matrix (see Table I). Figure 3(c) shows the crosssection of the 10 wt% Bi<sub>2</sub>O<sub>3</sub>-added indialite substrate with an average thickness of 500 μm, which was sintered at 900 °C. Figure 3(d) shows the magnified view of the substrate showing the high-density sintering of the indialite dark and Bi<sub>2</sub>SiO<sub>5</sub> bright phases without pores.

Figure 4(a) shows the dielectric properties of the 10 wt% Bi<sub>2</sub>O<sub>3</sub>-added indialite sintered at 900 °C in the frequency range of 100 Hz-1 MHz. Note that the developed substrates showed decreases in relative permittivity and dielectric loss with increasing frequency in the range from 100 Hz to 1 MHz. The substrates also showed an excellent low relative permittivity of 6.35 at 100 Hz and a decreased permittivity of 6.10 at 1 MHz. This relative permittivity is higher than that expected for pure indialite because of the existing secondary Bi<sub>2</sub>SiO<sub>5</sub> phase. There was no report on the

dielectric properties of  $\text{Bi}_2\text{SiO}_5$  since it is a metastable phase.<sup>33)</sup> Similarly, the dielectric loss decreased from 0.01 to 0.0001 with the frequency. The dielectric loss of this proposed composition at 1 MHz is ultralow compared with the values reported for commercial LTCCs.<sup>35)</sup> The dielectric loss of the developed substrate is larger than that of indialite owing to the presence of a secondary phase, because a single phase is better than a composite.

Figure 4(b) shows the variations in dielectric properties at 1MHz in the measured temperature range of -40 to 100 °C. Note that relative permittivity and dielectric loss increased with temperature. The relative permittivity variation was about 1.6%, while dielectric loss variation ranged from 0.00002 to 0.002. The developed low-temperature sintering substrate exhibited a temperature coefficient of relative permittivity ( $TC\varepsilon$ ) of about 118 ppm/°C. The low-temperature-sintered substrate with  $\varepsilon_r = 6.10$  and  $\tan\delta = 0.00014$  at 1MHz is an ideal candidate for LTCC applications. Figure 5 shows the thermal expansion ( $CTE$ ) of 3.5 ppm/°C at 100 to 600 °C, which is lower values than those of other materials such as alumina (8.1 ppm/°C) and quartz (8-14 ppm/°C).  $TCf$  was calculated to be -62.5 ppm/°C using the equation  $TCf = -[TCE + TC\varepsilon/2]$ .<sup>36)</sup> This paper is the first step towards new low permittivity and dielectric loss, and new LTCC substrates even for higher frequency solutions.

#### 4. Conclusions

A novel low-temperature-sintered microwave dielectric material with  $\varepsilon_r = 6.10$  and  $\tan\delta = 0.0001$  at 1 MHz was developed using 10 wt%  $\text{Bi}_2\text{O}_3$  added indialite powder crystallized at 1200 °C for 1 h. The material composed of indialite and  $\text{Bi}_2\text{SiO}_5$  was sintered at a relative density of 97%. A low-temperature sintering substrate was fabricated using a cast green tape with 10 wt%  $\text{Bi}_2\text{O}_3$ -added indialite with a binder and plasticizers, followed by thermo-lamination and sintering. The developed substrate showed a low relative permittivity of 6.10, an ultralow dielectric loss of 0.00014, and a  $TC\varepsilon$  of 118 ppm/°C at 1 MHz. They also showed a  $CTE$  of 3.5 ppm/°C in the measured temperature

range of 100-600 °C. The developed substrate for LTCC suggests that it might be an ideal choice for radio frequency applications.

### **Acknowledgements**

The authors are thankful to Professor Isao Kagomiya of Nagoya Institute of Technology, Professors Hiroataka Ogawa and Akinori Kan of Meijo University, and President Sadahiko Suzuki of Marusu Glaze Co., Ltd. for the preparation of the indialite/cordierite powder. Dr. Hitoshi Ohsato is grateful to JSPS KAKENHI Grant Number JP16K06735 and Nokia Foundation 2016 for supporting this work for Nokia Visiting Professors Project 201700003. Professor Heli Jantunen and Dr. Jobin Varghese are grateful to European Research Council Project No. 24001893 for financial assistance.

## References

1. M. T. Sebastian, and H. Jantunen, *Int. Mater. Rev.* **53**, 57 (2008).
2. J. Varghese, *Zircon Based Hard, Soft Microwave Substrates, and Devices* (Lambert Academic, Moldova, 2017) Chap. 1.
3. M. T. Sebastian, and H. Jantunen, in *Microwave Materials and Applications* ed. M. T. Sebastian, R. Uvic, and H. Jantunen (Wiley, New York, 2017) Vol. 1, Chap. 8.
4. A. Rydosz, W. Maziarz, J. Pisarkiewicz, H. Bartsch, and J. Muller, *Int. J. Inf. Electr. Eng.* **6**, 143 (2016).
5. S. Bierlich, T. Reimann, St. Barth, B. Caprato, H. Bartsch, J. Muller, and J. Topfer, *Int. J. Appl. Ceram. Technol.* **13**, 540 (2016).
6. D. Thomas, P. Abhilash, and M. T. Sebastian, *J. Eur. Ceram. Soc.* **33**, 87 (2013).
7. P. Abhilash, M. T. Sebastian, and K. P. Surendran, *J. Eur. Ceram. Soc.* **35**, 2313 (2015).
8. S. Arun, M.T. Sebastian, and K.P. Surendran, *Ceram. Intr.* **43**, 5509 (2017).
9. I. J. Induja, K. P. Surendran, M. R. Varma, and M. T. Sebastian, *Ceram. Intr.* **43**, 736 (2017).
10. G. Subodh, and M. T. Sebastian, *J. Amer. Ceram. Soc.* **90**, 2266 (2007).
11. J. Honkamo, H. Jantunen, G. Subodh, M. T. Sebastian, and P. Mohanan, *Intr. J. Appl. Ceram. Tech.* **6**, 531 (2009).
12. G. Subodh, and M. T. Sebastian, *Jpn. J. Appl. Phys.* **47**, 7943 (2008).
13. A. N. Unnimaya, E. K. Suresh, and R. Ratheesh. *Mater. Res. Bull.* **88**, 174 (2017).
14. E. K. Suresh, K. Prasad, N. S. Arun, and R. Ratheesh. *J. Electron. Mater.* **45**, 2996 (2016).
15. M. Ando, H. Ohsato, D. Igimi, Y. Higashida, A. Kan, S. Suzuki, Y. Yasufuku, and I. Kagomiya, *Jpn. J. Appl. Phys.* **54**, 10NE03 (2015).
16. H. Ohsato, *J. Ceram. Soc. Jpn.* **113**, 703 (2005).
17. H. Ohsato, *MRS Proc.* **833**, 55 (2005).



18. H. Ohsato, T. Tsunooka, M. Ando, Y. Ohishi, Y. Miyauchi, and K. Kakimoto, *J. Korean Ceram. Soc.* **40**, 350 (2003).
19. N. Kostylev, M. Goryachev, A. D. Bulanov, V. A. Gavva, and M. E. Tobar, *Sci. Rep.* **7**, 44813 (2017).
20. M. Terada, K. Kawamura, I. Kagomiya, K. Kakimoto, and H. Ohsato, *J. Eur. Ceram. Soc.* **27**, 3045 (2007).
21. H. Ohsato, M. Terada, and K. Kawamura, *Jpn. J. Appl. Phys.* **51**, 09LF02 (2012).
22. I. Kagomiya, I. Suzuki, and H. Ohsato, *Jpn. J. Appl. Phys.* **48**, 09KE02 (2009).
23. H. Ohsato, I. Suzuki, and I. Kagomiya, *Mater. Res. Bull.*, In press, December (2016) DOI: 10.1016/j.materresbull.2016.12.020.
24. M. Ando, K. Himura, T. Tsunooka, I. Kagomiya, and H. Ohsato, *Jpn. J. Appl. Phys.* **46**, 7112 (2007).
25. M. Ando, H. Ohsato, I. Kagomiya, and T. Tsunooka, *Jpn. J. Appl. Phys.* **47**, 7729 (2008).
26. T. Tsunooka, M. Ando, S. Suzuki, Y. Yasufuku, and H. Ohsato, *Jpn. J. Appl. Phys.* **52**, 09KH02 (2013).
27. T. Tsunooka, H. Sugiyama, K. Kakimoto, H. Ohsato, and H. Ogawa, *J. Ceram. Soc. Jpn.* **112**, S1637 (2004).
28. H. Ohsato, M. Ando, and T. Tsunooka, *J. Korean Ceram. Soc.* **44**, 597 (2007).
29. H. Ohsato, J. S. Kim, A.Y. Kim, C. I. Cheon, and K.W. Chae, *Jpn. J. Appl. Phys.* **50**, 09NF01 (2011).
30. H. Ohsato, in *Microwave Materials and Applications*, ed. M.T. Sebastian, R. Uvic, and H. Jantunen (Wiley, New York, 2017) Vol. 1, Chap. 5.
31. H. Ohsato, J. S. Kim, C. I. Cheon, and I. Kagomiya, *Ceram. Inter.* **41**, S588 (2015).
32. R. M. German, P. Suri, and S. J. Park, *J. Mater. Sci.* **44**, 1, (2009).

33. Y. T. Fei, S. J. Fan, R. Y. Sun, and M. Ishii, *Prog. Cryst. Growth Charact. Mater.* **40**, 183 (2000).
34. R. E. Mistler, and E. R. Twiname, *Tape Casting, Theory and Practice* (American Ceramic Society, Westerville, OH, 2000) Appendix 1.
35. <http://www.murata.com/~media/webrenewal/support/library/catalog/products/substrate/ltcc/n20e.ashx> (Accessed June 27, 2017).
36. M. T. Sebastian, *Dielectric Materials for Wireless Communications* (Elsevier, Amsterdam, 2008) Chapter 1.

## Table and figure captions

Table I Tape casting slurry composition.

Fig. [1.] (Color online) X-ray diffraction patterns (a), dielectric properties of indialite added with 5, 10, 15, and 20 wt%  $\text{Bi}_2\text{O}_3$  after sintering at 900 °C (b), and densification of indialite with 10 wt%  $\text{Bi}_2\text{O}_3$  at different sintering temperatures (c) with inset representing backscattering image of the 10 wt%  $\text{Bi}_2\text{O}_3$ -added sample after sintering at 900 °C/2 h.

Fig. [2.] (Color online) Photograph of cast green tape (a), five-layer laminated multilayer substrate (b), and sintered substrate at 900 °C (c).

Fig. [3.] (Color online) Cross-sectional microstructure of 10 wt%  $\text{Bi}_2\text{O}_3$ -added indialite green single-layer tape (a) and its magnified view (b), and cross section of a five-layer sample sintered at 900 °C (c) and its magnified view (d).

Fig. [4.] Variation in relative permittivity and dielectric loss tangent as a function of frequency (a), and temperature at 1 MHz (b).

Fig. [5.] Thermal expansion of 10 wt%  $\text{Bi}_2\text{O}_3$ -added indialite substrate as a function of temperature.

Table I

<b>Materials</b>	<b>Composition (wt%)</b>
Indialite+10 wt% Bi <sub>2</sub> O <sub>3</sub>	55
Xylene/ethanol (1:1)	(18.75 : 18.75)
Fish oil	1.4
PVB	4
BBP	1
PEG	1

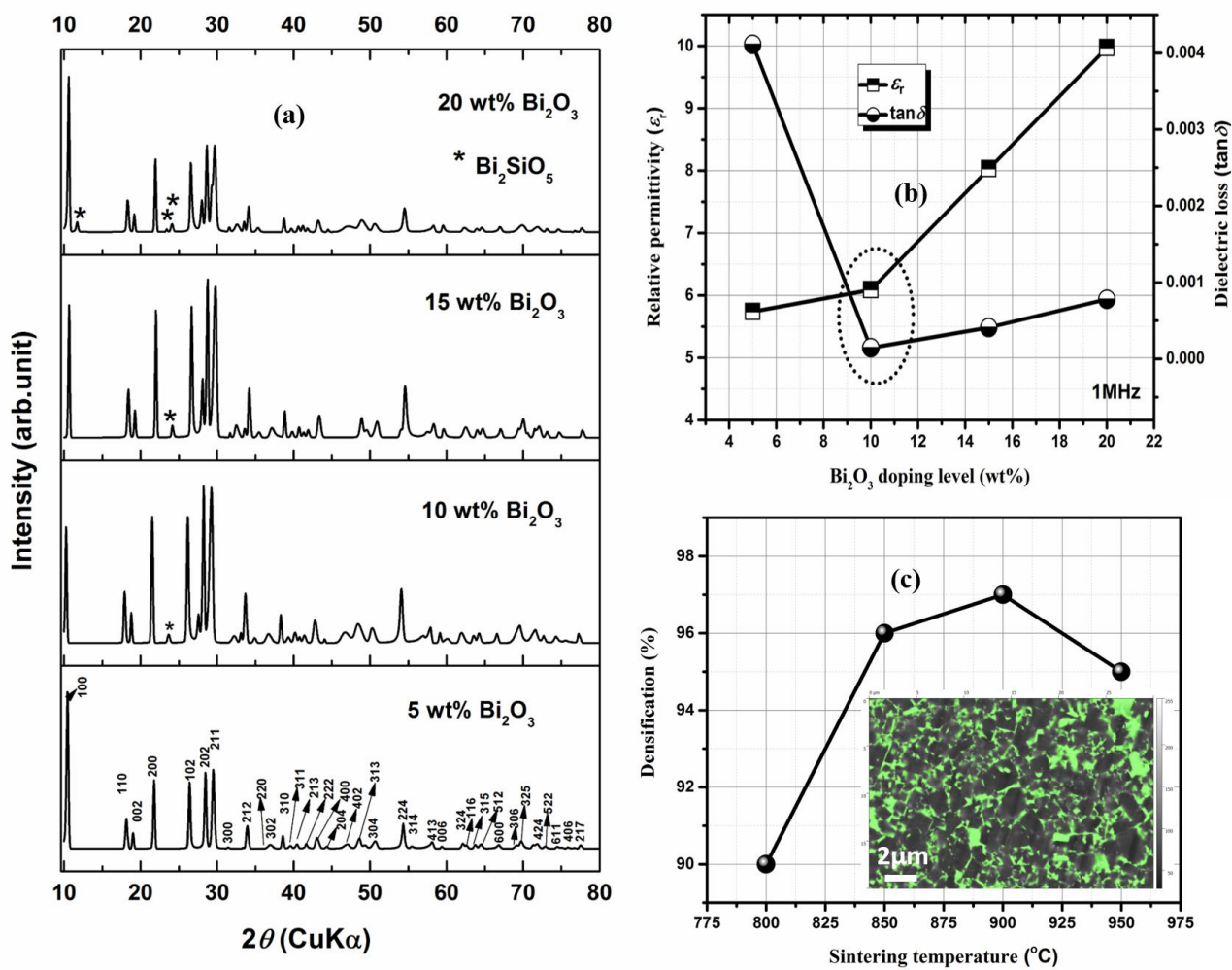


Fig. 1

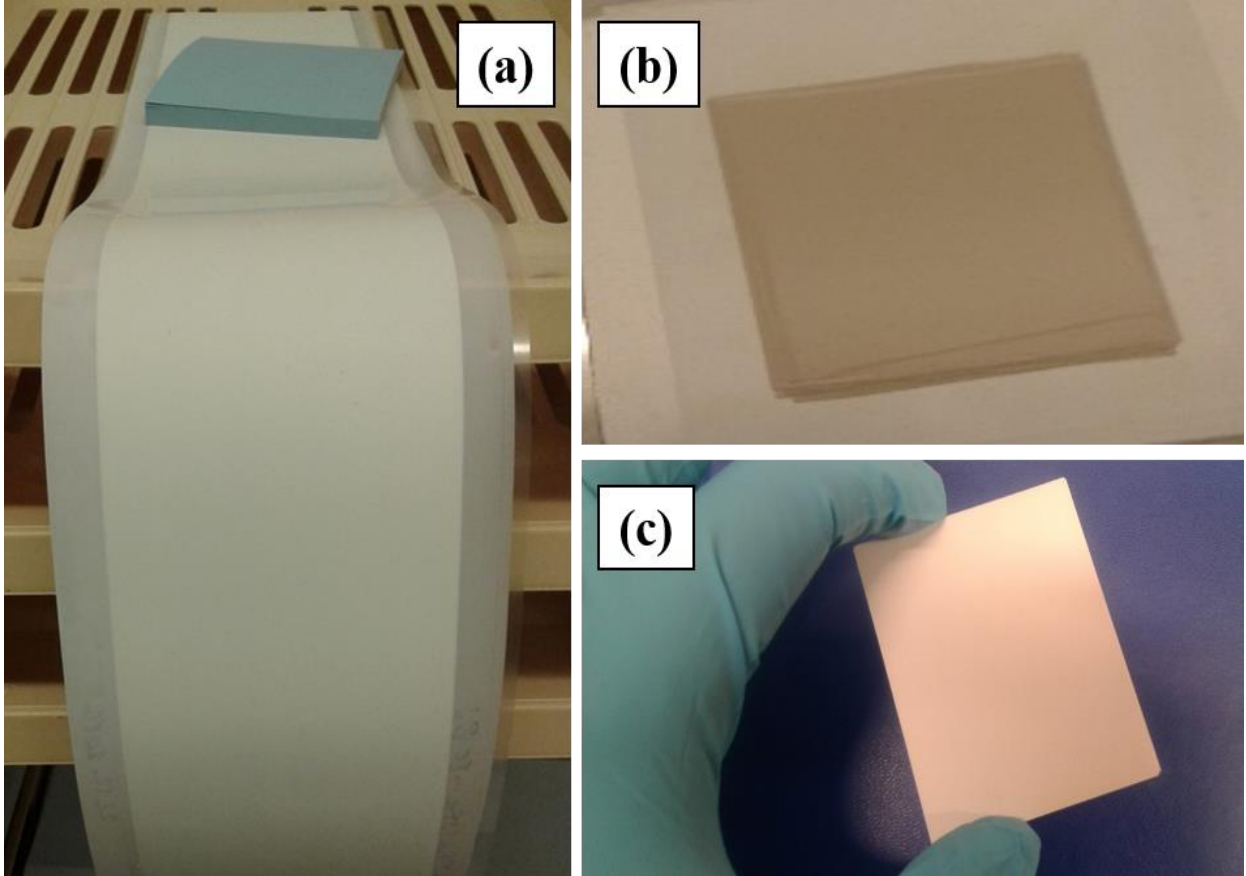


Fig. 2

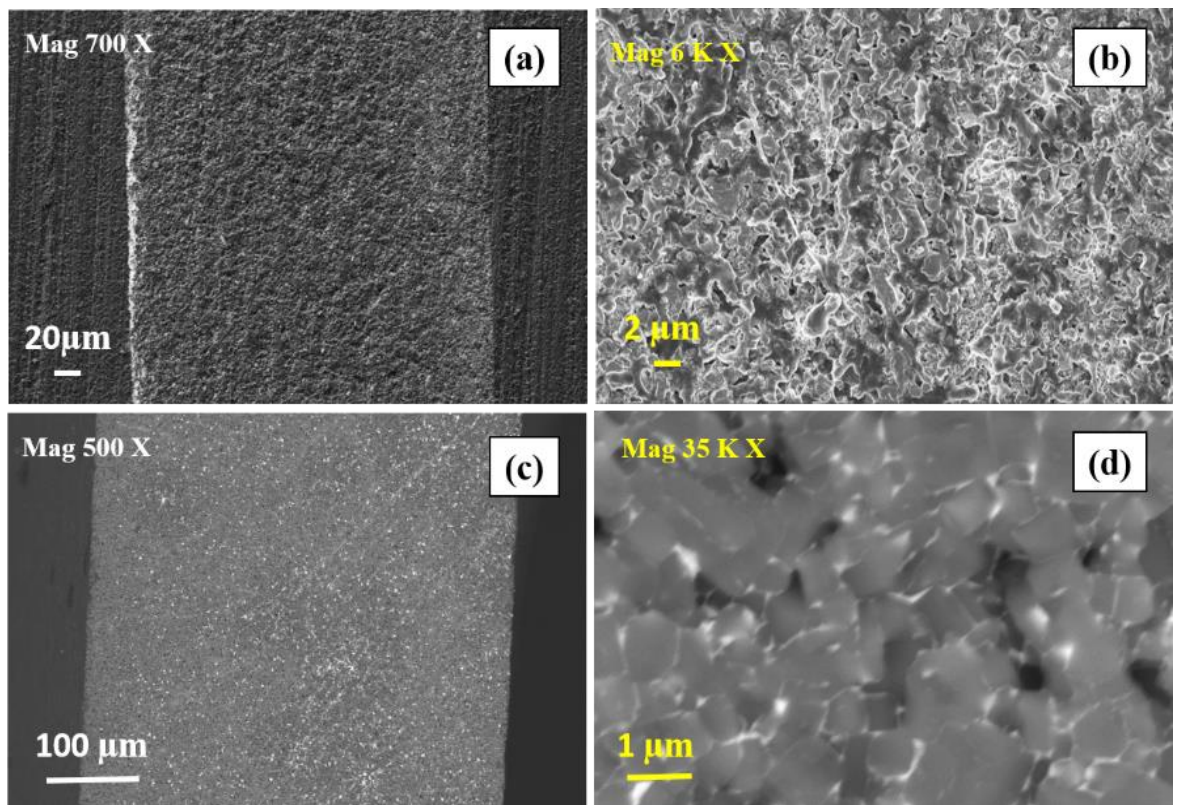


Fig. 3

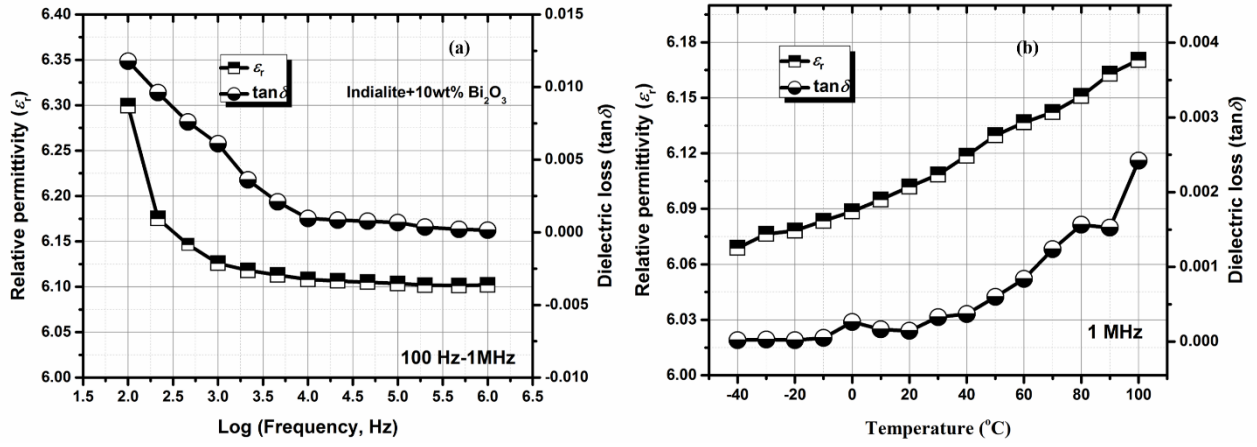


Fig. 4



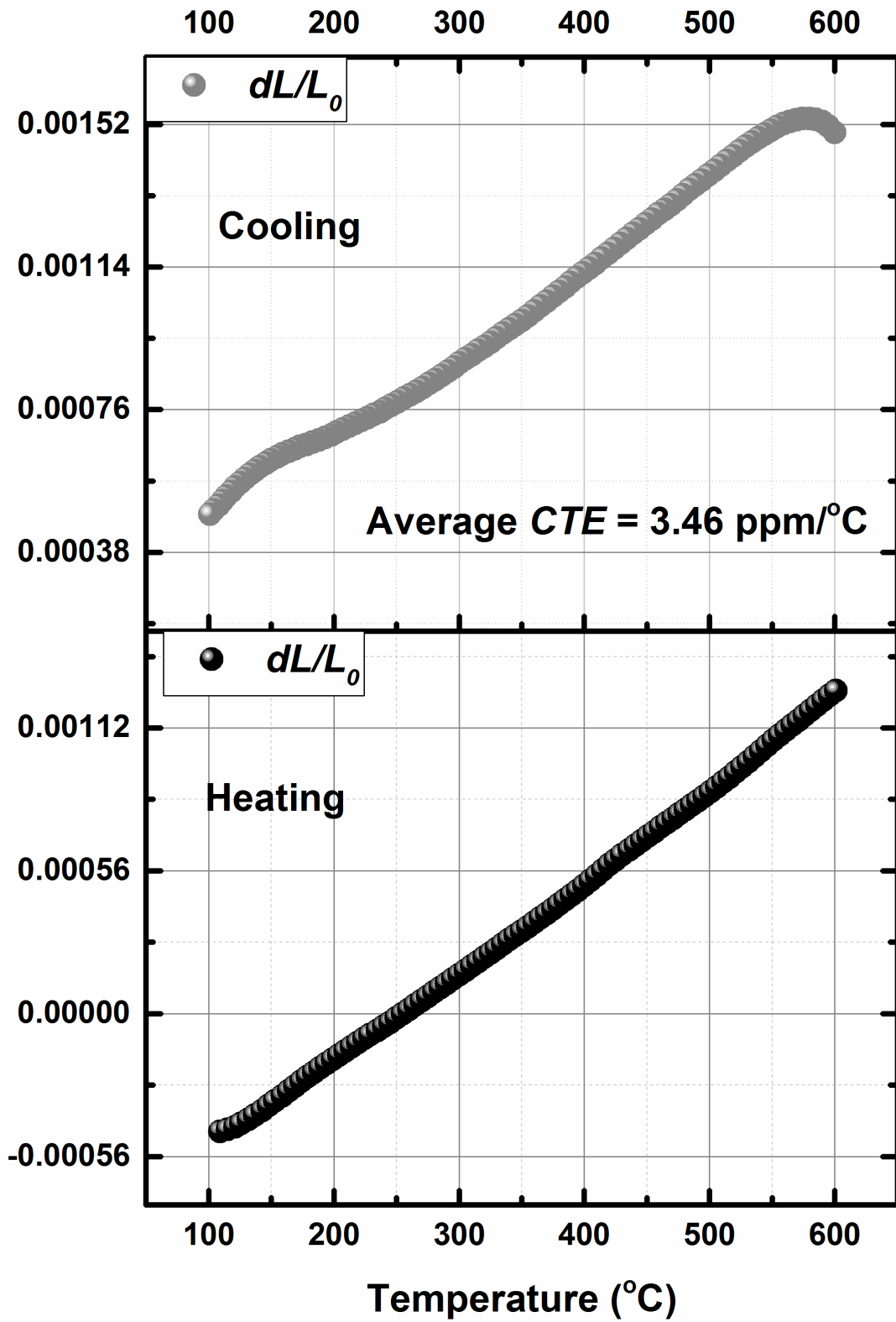


Fig. 5

